Am J Cancer Res 2021;11(12):6060-6073
www.ajcr.us /ISSN:2156-6976/ajcr0138677

Original Article

MIEAP, a p53-downstream gene, is associated with suppression of breast cancer cell proliferation and better survival

Manabu Futamura[1*], Yoshihisa Tokumaru[1*], Kazuaki Takabe[2], Hirofumi Arakawa[3], Yoshimi Asano[1], Ryutaro Mori[1], Junichi Mase[1], Akira Nakakami[1], Kazuhiro Yoshida[4]

[1]Breast Surgery, Department of Surgery, Graduate School of Medicine, Gifu University, 1-1 Yanagido, Gifu 501-1194, Japan; [2]Breast Surgery, Department of Surgical Oncology, Roswell Park Comprehensive Cancer Center, Buffalo, NY 14263, USA; [3]Division of Cancer Biology, National Cancer Center Research Institute, 5-1-1 Tsukiji, Chuo-ku, Tokyo 104-0045, Japan; [4]Gastroenterological Surgery, Department of Surgery, Graduate School of Medicine, Gifu University, 1-1 Yanagido, Gifu 501-1194, Japan. [*]Equal contributors.

Received August 28, 2021; Accepted October 19, 2021; Epub December 15, 2021; Published December 30, 2021

Abstract: Mitochondria-eating protein (*MIEAP*; also known as *SPATA18*), a p53-downstream gene, is involved in mitochondrial quality control (MQC). Enforced MIEAP expression induces caspase-dependent cell death in vitro, and impairment of the p53/*MIEAP*-regulated MQC pathway is frequently observed in breast cancer (BC), resulting in poor disease-free survival (DFS). To investigate the clinical significance of *MIEAP* in BC, we identified 2,980 patients from two global, large-scale primary BC cohorts: the Molecular Taxonomy of Breast Cancer International Consortium (METABRIC; n=1,904) and the Cancer Genome Atlas (TCGA; n=1,076). We divided patients in each cohort into high and low groups based on median gene expression levels and analyzed the association between *MIEAP* expression and clinical outcomes. Compared with normal tumors, *MIEAP* expression was significantly downregulated in all patients with *p53*-mutant BC regardless of subtype. *MIEAP* expression was negatively correlated with *KI67* expression. Gene set enrichment analysis demonstrated that cell cycle- and proliferation-associated gene sets were significantly enriched in *MIEAP*-low tumors compared to *MIEAP*-high tumors. Patients with *MIEAP*-high luminal subtype were associated with significantly longer DFS than those with *MIEAP*-low luminal tumors in both cohorts, whereas significantly longer overall survival was observed only in the METABRIC cohort, which has roughly double the number of samples. These results indicated that the mechanistic role of *MIEAP* is clinically relevant in the two independent cohorts. This is the first study to use large cohorts to demonstrate the association between *MIEAP* expression and survival in patients with luminal subtype BC.

Keywords: *MIEAP*, p53-downstream gene, breast cancer, prognosis, METABRIC, TCGA

Introduction

TP53, known as the most mutated tumor suppressor gene, works as a transcription factor in response to DNA damage [1]. p53 induces various kinds of downstream genes associated with cell cycle arrest, apoptosis, anti-angiogenesis, and DNA repair, among others [2-8]. Our group has isolated and characterized many p53-downstream genes using various cancer cell lines to elucidate the underlying mechanism of tumor suppression. *In vitro* studies showed the direct physical binding of p53 to the p53-binding site in the promoter region and consequent transcriptional activation [9, 10]. Although accumulating evidence has clarified the physiological function of p53 as a tumor suppressor, the clinical significance of each gene has not been sufficiently investigated.

We reported that the mitochondria-eating protein (*MIEAP*), also known as *SPATA18*, is a p53-downstream gene involved in mitochondrial quality control (MQC) [11, 12].

Mitochondria are pivotal intracellular organs for ATP synthesis, reactive oxygen species (ROS) production, apoptosis, and unfolded protein (UP) response [13-15]. Dysfunctional mitochondria may cause metabolic disorders such as a

higher rate of glycolysis in cancer cells, known as the Warburg effect [16, 17]. We found that MIEAP maintains healthy mitochondria under various physical conditions. When the cells suffer from slight mitochondrial damage, ATP synthesis is decreased, and ROS production is increased. Under these conditions, MIEAP is induced and operates to recover mitochondria with co-factors such as BCL2/adenovirus E1B 19 kDa protein-interacting protein 3 (BNIP3) and BCL2/adenovirus E1B 19 kDa protein-interacting protein 3-like (BNIP3L, also known as NIX) [18]. We call this phenomenon the MIEAP-induced accumulation of lysosome-like organelles within mitochondria (MALM). However, when mitochondrial damage is severe, MIEAP degrades damaged mitochondria by a vacuole-like structure called MIEAP-induced vacuole (MIV) [12]. These findings suggest that MIEAP may play a role in the Warburg effect, through the p53/*MIEAP*-regulated pathway.

Breast cancer (BC) is a frequently occurring cancer in women worldwide, and elucidation of its molecular mechanism is essential for developing novel treatments [19]. To investigate the clinical significance of *MIEAP* in BC, we previously analyzed surgically dissected tissues and found that 26% of patients had impaired p53/*MIEAP*-regulated MQC pathways, resulting in a shorter disease-free survival (DFS) [20]. Besides, immunohistochemistry (IHC) demonstrated a lower positive rate of *MIEAP* expression in invasive ductal carcinoma than in benign tumors or non-invasive carcinoma [20]. Therefore, we assume that *MIEAP* plays a critical role clinically in the malignant transformation of breast tumors.

In this study, we aimed to investigate our hypothesis that *MIEAP* is a p53-regulated tumor suppressive gene associated with cancer prognosis *in vivo* using two worldwide large-scale primary BC cohorts: the Molecular Taxonomy of Breast Cancer International Consortium (METABRIC) [21] and the Cancer Genome Atlas (TCGA) [22].

Materials and methods

Cohorts and patients

We performed this study using two independent large-scale BC cohorts: the METABRIC cohort, which consists mainly of patients from the United Kingdom and Canada [21], and the TCGA cohort, which consists mainly of patients from the United States [22]. Both cohort databases are publicly available and easily accessible. Clinicopathological and genomic/gene expression data from 1,076 patients in the TCGA cohort and 1,904 patients in the METABRIC cohort were downloaded from cBioPortal, as previously described. The receptor status was obtained from clinical parameters by IHC. AJCC cancer staging, and pathological analysis were used according to the Nottingham pathological grade. We obtained 1,336 and 584 luminal, 236 and 182 HER2+, as well as 267 and 157 TN subtypes from the METABRIC cohort and the TCGA cohort, respectively (**Table 1**). We divided the patients in each cohort into high and low groups based on median gene expression levels (Figure S1) and analyzed the association between *MIEAP* expression and clinical outcome. The Kaplan-Meier method with the log-rank test was used to compare the survival curves between *MIEAP*-high and *MIEAP*-low tumors. DFS was defined from the time of primary treatment to clinical tumor recurrence. OS was defined as the time to death from BC. Patients who died from other causes were excluded from the study. Furthermore, expression data for metastatic BC (GSE110590) were obtained from the Gene Expression Omnibus (GEO) of the National Center for Biotechnology Information (NCBI; https://www.ncbi.nlm.nih.gov). As all data used in this study were publicly available and de-identified, the requirement for approval of the Institutional Review Board was waived.

Gene set enrichment analysis (GSEA)

GSEA, a computational method to determine whether a defined set of genes is statistically significant, was performed on the data from the METABRIC and TCGA cohorts using GSEA software (http://software.broadinstitute.org/gsea/index.jsp; Broad Institute, Cambridge, MA, USA) as described previously [23-26]. For expression analysis, we classified patients into two groups based on *MIEAP* expression using the median of the gene expression range. An FDR<0.25 was considered statistically significant based on the recommendation of the software developer.

Table 1. Clinicopathological demographic data of the *MIEAP*-high and *MIEAP*-low groups

A			
Clinicopathological factors	TCGA whole cohort (n=1076)		
	MIEAP-high n=538	*MIEAP*-low n=538	*P* value
Age			
<65 y	337	363	0.357
≥65 y	160	175	
Unknown	1	0	
ER status			
Positive	455	337	<0.001
Negative	56	178	
Unknown	27	23	
PR status			
Positive	409	276	<0.001
Negative	100	238	
Unknown	29	24	
HER2 status			
Positive	71	111	0.003
Negative	389	366	
Unknown			
Stage			
I/II/III/IV	94/300/121/10	84/310/12/9	0.837
Unknown	13	10	
pT			
T1/T2/T3/T4	258/178/55/39	250/176/64/36	0.704
Tx	1	1	
pN			
N0/N1/N2/N3	258/178/55/39	250/176/64/36	0.819
M			
M0/M1	442/10	454/11	1
Mx	86	73	
B			
Clinicopathological factors	METABTIC whole cohort (n=1904)		
	MIEAP-high n=952	*MIEAP*-low n=952	*P* value
Age			
<65 y	542	575	0.136
≥65 y	410	377	
Unknown	0	0	
ER status			
Positive	843	602	<0.001
Negative	94	336	
Unknown	15	14	
PR status			
Positive	643	366	<0.001
Negative	309	586	
Unknown	0	0	

Statistical analysis

The clinicopathological findings were compared using the chi-squared test, Fisher's exact test, or Student's t-test. The differences in DFS and OS between *MIEAP*-high and *MIEAP*-low tumors were analyzed using the Kaplan-Meier method with the log-rank test. Statistical significance was defined at $P<0.05$. Spearman's correlation was used for identifying significant associations. Statistical analysis was carried out using Microsoft Excel 2016, R (http:///www.r-project.org/), and Bioconductor (http://bioconductor.org/).

Results

MIEAP expression is associated with TP53 status

MIEAP has been shown to be downstream of p53. As METABRIC and TCGA contain data on both gene expression and genomic DNA, we investigated the relationship between *TP53* status and *MIEAP* expression. Based on both cohorts, *MIEAP* expression was significantly higher in patients with BC (ER+HER2-, HER2+, ER+HER2, and triple-negative [TN]) with wild-type (wt) *TP53* than in those with mutant (mut) *TP53* for both cohorts (**Figure 1A**). These results indicate that *MIEAP* expression is dependent on *TP53* status.

MIEAP is downregulated in BC tissues, particularly in metastatic sites

As *MIEAP* is a tumor suppressor regulated by p53, we speculated that *MIEAP* might be downregulated in tumor tissues. We compared *MIEAP* expression in tumor tissues with that in normal tissues. Based on the TCGA data-

HER2 status			
Positive	50	186	<0.001
Negative	902	586	
Unknown	0	0	
Stage			
0/I/II/III/IV	1/283/390/43/4	3/192/410/72/5	<0.001
Unknown	231	270	
Tumor size			
≤2 cm	459	362	<0.001
2 cm-5 cm	427	495	
>5 cm	427	494	
Unknown	8	12	
LN metastasis			
Positive	418	493	<0.001
Negative	534	459	

Clinicopathological features were obtained from TCGA (A) and METABRIC (B). The patients were divided into high and low groups based on median gene expression levels in each cohort. ER: estrogen receptor, PR: progesterone receptor, HER2: human epidermal growth factor receptor 2, LN: Lymph node.

set, *MIEAP* expression was significantly lower in tumor tissues than in normal tissues (P<0.001) (**Figure 1B**). Based on the GSE110590 dataset, *MIEAP* expression was significantly lower in metastatic sites than in primary tumors (P=0.041). The metastatic sites were adrenal gland, axillary lymph node, brain, dura, kidney, liver, lung, pancreas, pleura, rib, skin, skull, spinal cord, and subcarinal lymph node (**Figure 1C**). These results suggest that *MIEAP* is downregulated as cancer progresses.

MIEAP expression is low in advanced American Joint Committee on Cancer (AJCC) clinical stage and/or advanced Nottingham pathological grade

We compared *MIEAP* expression with the AJCC clinical stage [27]. In the METABRIC cohort, *MIEAP* expression was significantly decreased as the clinical stage advanced in the whole cohort and the ER+/HER2- (luminal) subtype (P<0.001 and P=0.003, respectively). However, no association was found in the TCGA cohort (**Figure 2A**). We also observed that the number of ER+/HER2- patients in the *MIEAP*-high groups was higher than that in the *MIEAP*-low groups (**Table 1**). In the *MIEAP*-high group, there were many patients with either ER+, PR+, HER2-, small tumor, or no lymph node metastasis in the METABRIC cohort and many patients with ER+ and/or PR+ in the TCGA cohort. Next, we compared *MIEAP* expression with the Nottingham pathological grade [28]. In the METABRIC cohort, *MIEAP* expression was decreased as tumor grade advanced in the whole cohort (P<0.001) and the luminal and TN subtypes (P<0.001 and P=0.006, respectively). In the TCGA cohort, *MIEAP* expression was decreased as tumor grade advanced in the whole cohort (P<0.001) and the luminal subtype (P=0.004) (**Figure 2B**).

MIEAP expression is negatively correlated with KI67

As we speculated that *MIEAP* might be associated with tumor proliferation, we investigated the correlation between *MIEAP* expression and *KI67*, a cell proliferation marker. In the METABRIC cohort, a positive correlation was found in the whole cohort (r=0.336, P<0.01) and the luminal (r=0.23, P<0.01) and TN (r=0.176, P<0.01) subtypes. In the TCGA cohort, a positive correlation was found in the whole cohort (r=0.382, P<0.01) and the HR+/HER2- (r=0.281, P<0.01) and HER2+ (r=0.176, P=0.02) subtypes (**Figure 2C**).

Low expression of MIEAP is associated with cell cycle- and proliferation-related gene sets

Based on the association between *MIEAP* and *KI67*, we performed GSEA for the whole cohort and each subtype to identify gene sets that might be associated with *MIEAP* expression. In the METABRIC cohort, *MIEAP*-low tumors in the whole cohort were significantly enriched in cell cycle- and proliferation-related gene sets such as Myc Targets V1 (normalized enrichment score [NES], -1.62; false discovery rate [FDR], 0.015), Myc targets V2 (NES, -1.72; FDR, 0.007), E2F targets (NES, -1.68; FDR, 0.007), G2M checkpoint (NES, -1.69; FDR, 0.006), mitotic spindle (NES, -1.66; FDR, 0.006), and mTORC1 signaling (NES, -1.72; FDR, 0.002). In the TCGA cohort, *MIEAP*-low tumors in the whole cohort were significantly enriched in cell cycle- and proliferation-related gene sets such as Myc targets V1 (NES, -2.18; FDR, <0.001), Myc Targets V2 (NES, -2.04; FDR, 0.006), E2F targets (NES, -2.31; FDR, <0.001), G2M checkpoint (NES, -2.34; FDR, <0.001), mitotic spindle (NES, -1.73; FDR, 0.042), and mTORC1 signaling (NES, -2.20; FDR, <0.001). Each subtype,

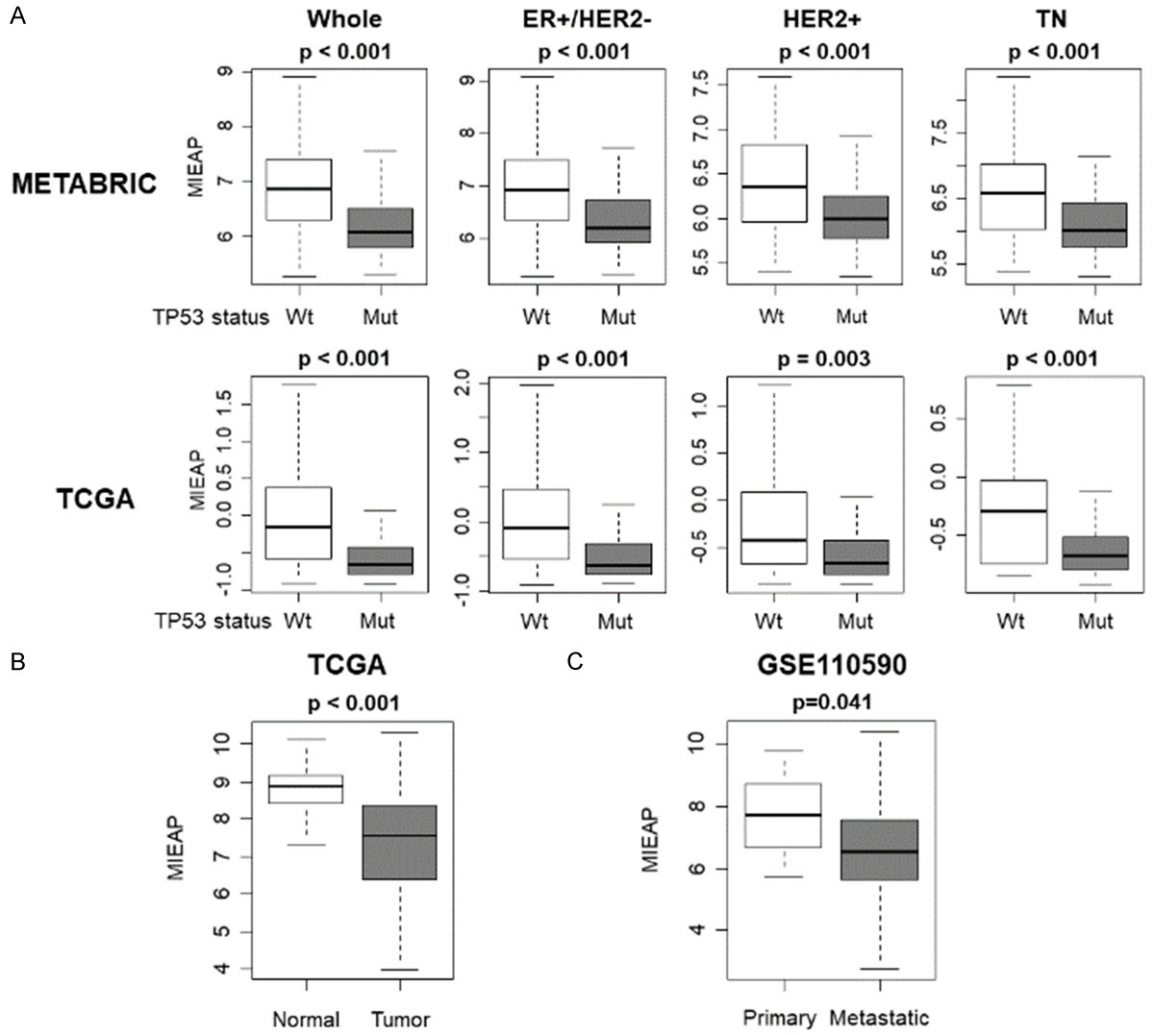

Figure 1. *MIEAP* expression is dependent on p53 status and is downregulated in tumor tissues. A. *MIEAP* expression depending on p53 status in each breast cancer subtype was demonstrated by METABRIC (*n*=1904) and TCGA (*n*=1076). Wt: wild-type, Mut: mutant, ER+: estrogen receptor positive, HER2: human epidermal growth factor receptor 2, TN: triple negative. B. Comparison of *MIEAP* expression in normal and tumor tissues by TCGA. C. Comparison of *MIEAP* expression in primary tumors (*n*=8) and metastatic tumors (*n*=51) by GSE110590.

but especially the luminal, in both cohorts was particularly enriched in the same gene sets (**Figure 3**). Most NES were negative in analyzing these gene sets. These results indicate that downregulation of *MIEAP* induces various genes associated with cell cycle and proliferation, leading to tumor progression.

MIEAP-high tumors are associated with favorable survival compared with MIEAP-low tumors

We previously reported that impairment of the p53/MIEAP-regulated MQC pathway in primary BCs resulted in poor DFS. We speculated that *MIEAP*-high tumors might result in a favorable prognosis [18]. To investigate the association between *MIEAP* expression and BC prognosis, we compared survival between *MIEAP*-high and *MIEAP*-low BC groups. In the METABRIC cohort, *MIEAP*-high BC demonstrated significantly favorable DFS and overall survival (OS) in the whole cohort and the luminal subtype (P<0.001 for all) (**Figure 4A**). In the TCGA cohort, *MIEAP*-high BC demonstrated significantly favorable DFS only in the luminal subtype (P=0.005) (**Figure 4B**).

MIEAP expression enrich mitochondria-related gene sets

We also performed GSEA for the whole cohort and each subtype to identify mitochondria-

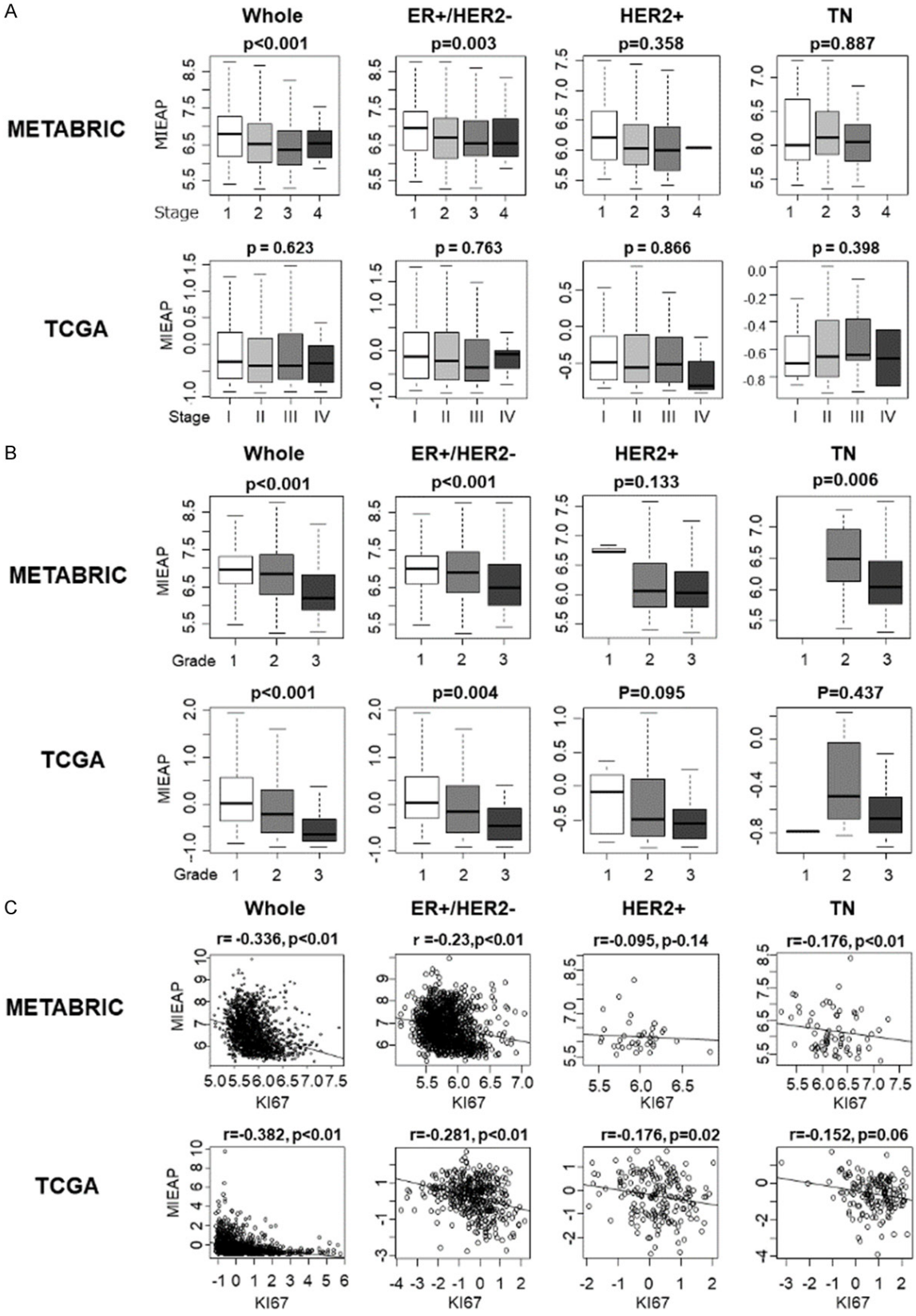

Figure 2. *MIEAP* expression based on clinical stage and pathological grade. *MIEAP* expression by AJCC cancer staging (A) and Nottingham pathological grade (B) by both the METABRIC and TCGA cohorts are shown. *MIEAP* expression was significantly downregulated as cancer stage and/or histological grade advanced. (C) Correlation between expression of *MIEAP* and *KI67* by METABRIC and TCGA.

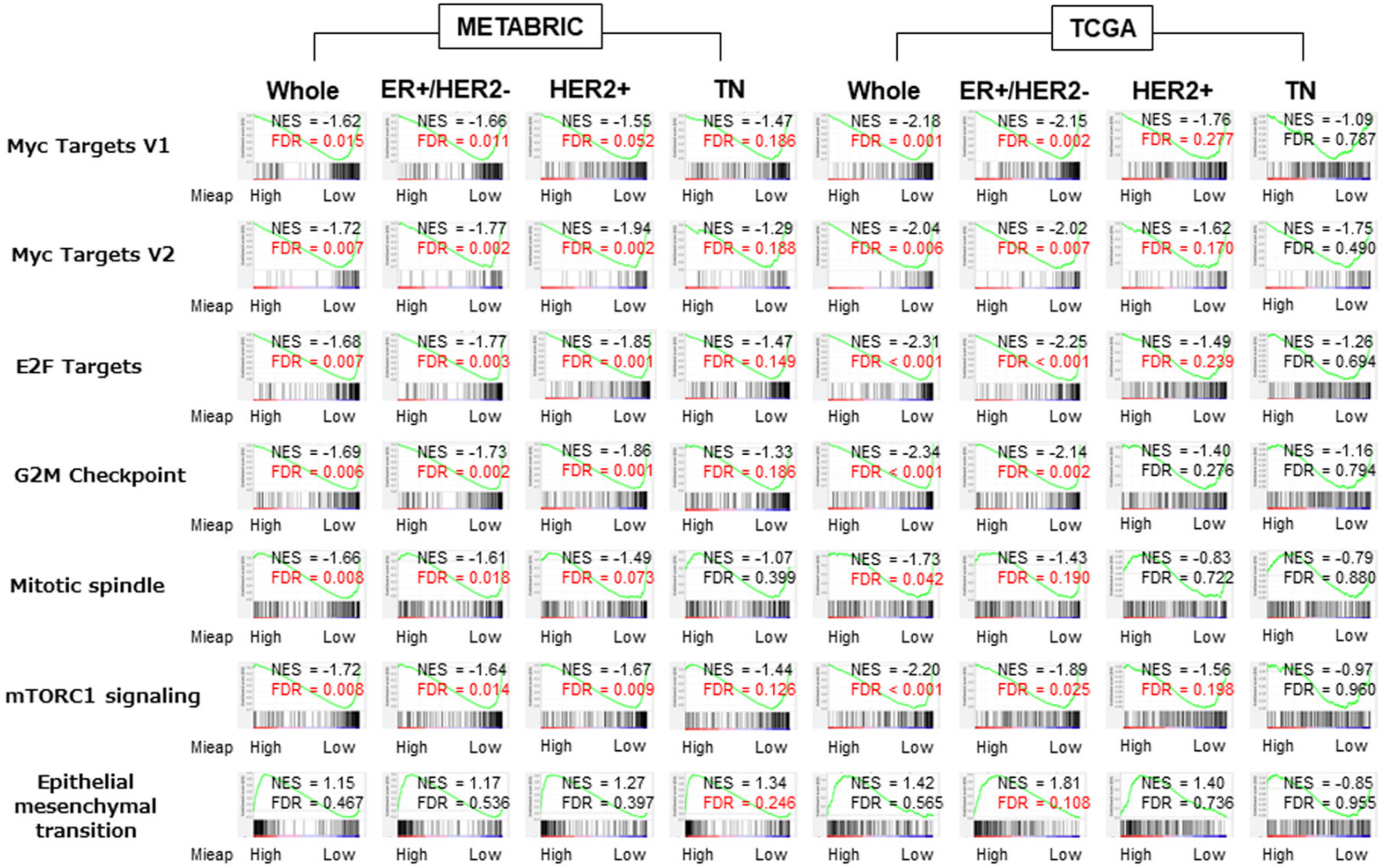

Figure 3. Gene set enrichment analysis (GSEA) of cell cycle- and proliferation-related gene sets from METABRIC and TCGA cohorts. Cell proliferation-related gene sets (Myc Targets V1, Myc Targets V2, and mTORC1 signaling), cell cycle-related gene sets (E2F Targets, G2M checkpoint, and mitotic spindle), and epithelial mesenchymal transition are shown. Normalized enrichment score (NES) and false discovery rate (FDR) are indicated. According to recommendation by the GSEA software, FDR<0.25 was considered statistically significant.

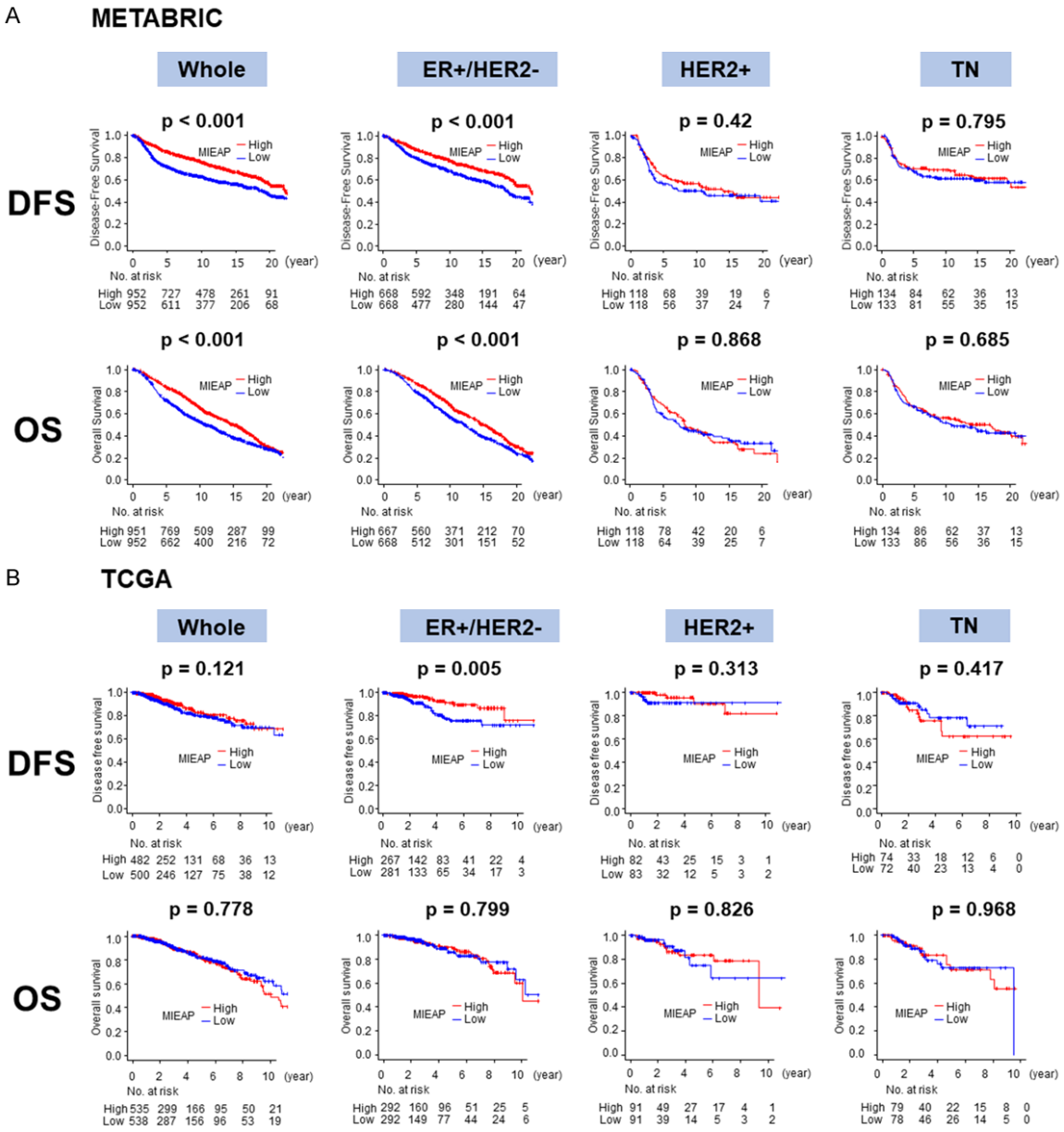

Figure 4. Overall survival (OS) and disease-free survival (DFS) of *MIEAP*-high expression group and *MIEAP*-low expression group. Kaplan-Meier analyses were performed in all subtypes by both cohorts. A median of the *MIEAP* expression was used to divide patients into low (blue) and high (red) expression groups. ER+: estrogen receptor positive, HER2: human epidermal growth factor receptor 2, TN: triple negative.

related gene sets that might be associated with MIEAP expression. In the METABRIC cohort, *MIEAP*-high tumors in the whole cohort were significantly enriched in the mitochondrial pathway (NES, -1.33; FDR, 0.215), oxidative phosphorylation (NES, -1.64; FDR, 0.065), glycolysis (NES, -1.76; FDR, 0.039), ROS pathway (NES, -1.37; FDR, 0.013), UP response (NES, -1.56; FDR, 0.103), activation of Noxa and translocation to mitochondria (NES, -1.51; FDR, 0.126), and electron transport reaction (ETR) pathway (NES, -1.41; FDR, 0.168). Besides, *MIEAP*-low tumors in the luminal subtype were significantly enriched in oxidative phosphorylation (NES, -1.76; FDR, 0.050), glycolysis (NES, -1.47, FDR, 0.173), and UP response (NES, -1.53; FDR, 0.142). In the TCGA cohort, *MIEAP*-low tumors in the whole cohort were significantly enriched in the ROS pathway (NES, -1.37; FDR, 0.103) and UP response (NES, -1.24; FDR, 0.026).

Besides, Mieap-high tumors in the TN subtype were significantly enriched in the mitochondrial pathway (NES, -1.43; FDR, 0.140), oxidative phosphorylation (NES, -1.24; FDR, 0.237), ROS pathway (NES, -1.33; FDR, 0.172), UP response (NES, -1.73; FDR, 0.173), and ETR pathway (NES, -1.49; FDR, 0.106) (**Figure 5**).

BNIP3 and NIX are downregulated in tumors and correlated with MIEAP

MIEAP has been demonstrated to functionally interact with *MIEAP*-associated co-factors such as BNIP3 and NIX (BNIP3L) [18]. An evaluation of the expression of these co-factors showed NIX to be significantly downregulated in tumor tissues ($P<0.001$), while BNIP3 was marginally downregulated ($P=0.051$) (**Figure 6A**). An analysis of the correlations between Mieap and co-factor molecules found a positive association ($P<0.01$) between *MIEAP* and *NIX* (METABRIC, $r=0.259$, $P<0.01$; TCGA, $r=0.301$, $P<0.01$). A positive correlation was also observed in ER+/HER2 ($r=0.171$, $P<0.01$) and HER2+ ($r=0.171$, $P<0.01$) subtypes (**Figure 6B**). However, no correlation between *MIEAP* and *BNIP3* was found in either the METABRIC or TCGA cohorts. Significant correlations with ER+/HER2- in METABRIC ($r=0.009$, $P<0.01$) and HER2+ in TCGA ($r=0.188$, $P=0.01$) were observed (**Figure 6C**).

Discussion

In our previous studies on p53-downstream genes, we isolated and characterized *MIEAP*, which regulates MQC with co-factors such as BNIP3 and NIX [18]. We also showed that *Mieap* deficiency in $Apc^{Min/+}$ mice increased the size and number of polyps, which demonstrated advanced grades of both adenoma and adenocarcinoma, resulting in a shorter lifetime [29]. These data suggest that *Mieap* is a tumor suppressor and is one of the pivotal molecules of the Warburg effect. Both *in vivo* and *in vitro* preclinical models are important tools to elucidate cancer biology; however, no model can perfectly mimic human cancer. Although our previous reports indicated the clinical relevance of *MIEAP* using surgically dissected specimens, the sample size was small, and thus, sampling bias might exist [20]. The novelty of the present study is the investigation of the clinical relevance of *MIEAP* using information from two worldwide large-scale primary BC cohorts. Several p53-downstream genes have been isolated and characterized thus far; nonetheless, the clinical relevance of these genes remains unclear owing to the difficulty in conducting a large-scale study using tumor samples. Our strategy involving the use of public large-scale cohorts is useful in characterizing these genes.

In the present study, we found that *MIEAP* was significantly downregulated in *TP53*-mut BC of all subtypes as cancer stage and/or histological grade advanced. Compared with normal tissues, *MIEAP* in all subtypes and the MIEAP co-factors *BNIP3* and *NIX* were significantly downregulated in tumors. *MIEAP* was reduced at various metastatic sites, as compared to primary tumors, and was negatively associated with *KI67*, suggesting that *MIEAP* is involved in cell proliferation. TP53-mutated tumors are well known to exhibit an aggressive phenotype and to be resistant to chemotherapeutic drugs [30]. We observed that not only TP53 alteration but also downregulation/impairment of p53-downstream genes can lead to an aggressive phenotype. These data suggest that MIEAP functions as a tumor suppressor that acts in cooperation with NIX and BNIP3. This is the first study to evaluate the association between TP53 status and expression of p53-downstream genes in large-scale cohorts. The results are consistent with our hypothesis that *MIEAP* is a p53-downstream tumor suppressor gene.

Our previous reports demonstrated that the impairment rates of the p53/*MIEAP*-regulated MQC pathway for gastric, esophageal, and colorectal cancers were 70.2%, 83.3%, and 79.5%, respectively, whereas that for BC was 26.1% [20, 31, 32]. The difference in impairment rates between gastrointestinal cancer (GIC) and BC could be attributed to the higher methylation rate of the BNIP3 promoter in the former than in the latter (30-40% in GIC vs. 0% in BC); however, the underlying mechanism remains unclear. We speculate that different regulatory mechanisms may exist for the expression of BNIP3 and NIX. Our previous studies demonstrated that enforced *MIEAP* induced NIX but not BNIP3 in BC and GIC cell lines, whereas our current data indicate that NIX has a stronger association with *MIEAP* than BNIP3 [20, 32].

According to our previous data, impairment of the p53/*MIEAP*-regulated MQC pathway leads

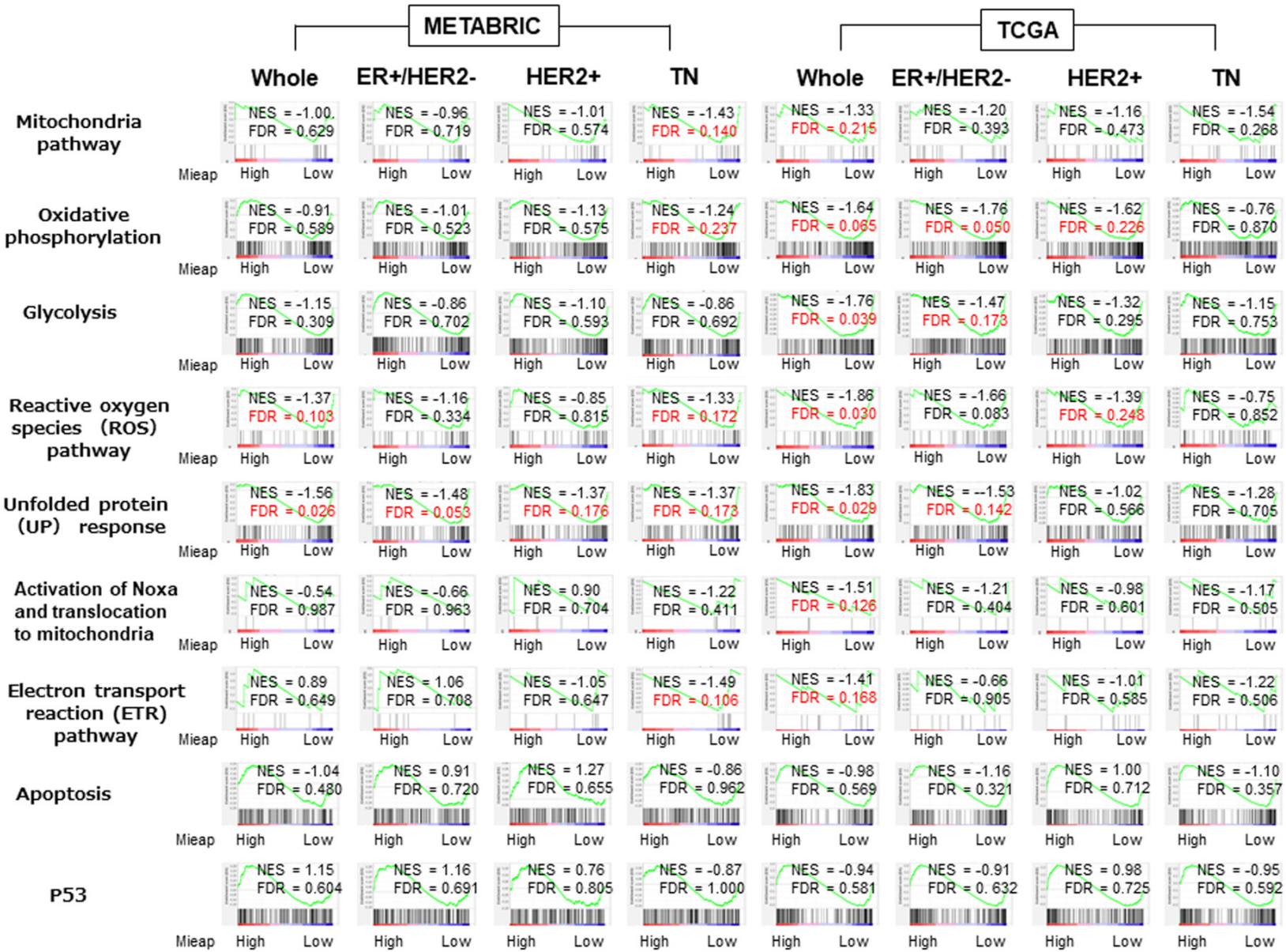
METABRIC
TCGA
Whole
ER+/HER2-
HER2+
TN
Whole
ER+/HER2-
HER2+
TN
Mitochondria pathway
NES = -1.00 FDR = 0.629
NES = -0.96 FDR = 0.719
NES = -1.01 FDR = 0.574
NES = -1.43 FDR = 0.140
NES = -1.33 FDR = 0.215
NES = -1.20 FDR = 0.393
NES = -1.16 FDR = 0.473
NES = -1.54 FDR = 0.268
Oxidative phosphorylation
NES = -0.91 FDR = 0.589
NES = -1.01 FDR = 0.523
NES = -1.13 FDR = 0.575
NES = -1.24 FDR = 0.237
NES = -1.64 FDR = 0.065
NES = -1.76 FDR = 0.050
NES = -1.62 FDR = 0.226
NES = -0.76 FDR = 0.870
Glycolysis
NES = -1.15 FDR = 0.309
NES = -0.86 FDR = 0.702
NES = -1.10 FDR = 0.593
NES = -0.86 FDR = 0.692
NES = -1.76 FDR = 0.039
NES = -1.47 FDR = 0.173
NES = -1.32 FDR = 0.295
NES = -1.15 FDR = 0.753
Reactive oxygen species (ROS) pathway
NES = -1.37 FDR = 0.103
NES = -1.16 FDR = 0.334
NES = -0.85 FDR = 0.815
NES = -1.33 FDR = 0.172
NES = -1.86 FDR = 0.030
NES = -1.66 FDR = 0.083
NES = -1.39 FDR = 0.248
NES = -0.75 FDR = 0.852
Unfolded protein (UP) response
NES = -1.56 FDR = 0.026
NES = -1.48 FDR = 0.053
NES = -1.37 FDR = 0.176
NES = -1.37 FDR = 0.173
NES = -1.83 FDR = 0.029
NES = --1.53 FDR = 0.142
NES = -1.02 FDR = 0.566
NES = -1.28 FDR = 0.705
Activation of Noxa and translocation to mitochondria
NES = -0.54 FDR = 0.987
NES = -0.66 FDR = 0.963
NES = 0.90 FDR = 0.704
NES = -1.22 FDR = 0.411
NES = -1.51 FDR = 0.126
NES = -1.21 FDR = 0.404
NES = -0.98 FDR = 0.601
NES = -1.17 FDR = 0.505
Electron transport reaction (ETR) pathway
NES = 0.89 FDR = 0.649
NES = 1.06 FDR = 0.708
NES = -1.05 FDR = 0.647
NES = -1.49 FDR = 0.106
NES = -1.41 FDR = 0.168
NES = -0.66 FDR = 0.905
NES = -1.01 FDR = 0.585
NES = -1.22 FDR = 0.506
Apoptosis
NES = -1.04 FDR = 0.480
NES = 0.91 FDR = 0.720
NES = 1.27 FDR = 0.655
NES = -0.86 FDR = 0.962
NES = -0.98 FDR = 0.569
NES = -1.16 FDR = 0.321
NES = 1.00 FDR = 0.712
NES = -1.10 FDR = 0.357
P53
NES = 1.15 FDR = 0.604
NES = 1.16 FDR = 0.691
NES = 0.76 FDR = 0.805
NES = -0.87 FDR = 1.000
NES = -0.94 FDR = 0.581
NES = -0.91 FDR = 0. 632
NES = 0.98 FDR = 0.725
NES = -0.95 FDR = 0.592
Mieap
High
Low

Figure 5. Gene set enrichment analysis (GSEA) of mitochondria- and *MIEAP*-related gene sets from METABRIC and TCGA cohorts. Mitochondria-related gene sets (mitochondria pathway, oxidative phosphorylation, glycolysis, reactive oxygen species pathway, unfolded protein response, activation of Noxa and translocation to mitochondria, electron transport reaction pathway) and p53-related pathway (apoptosis, p53) are shown. Normalized enrichment score (NES) and false discovery rate (FDR) are indicated. According to recommendation by the GSEA software, FDR<0.25 was considered statistically significant.

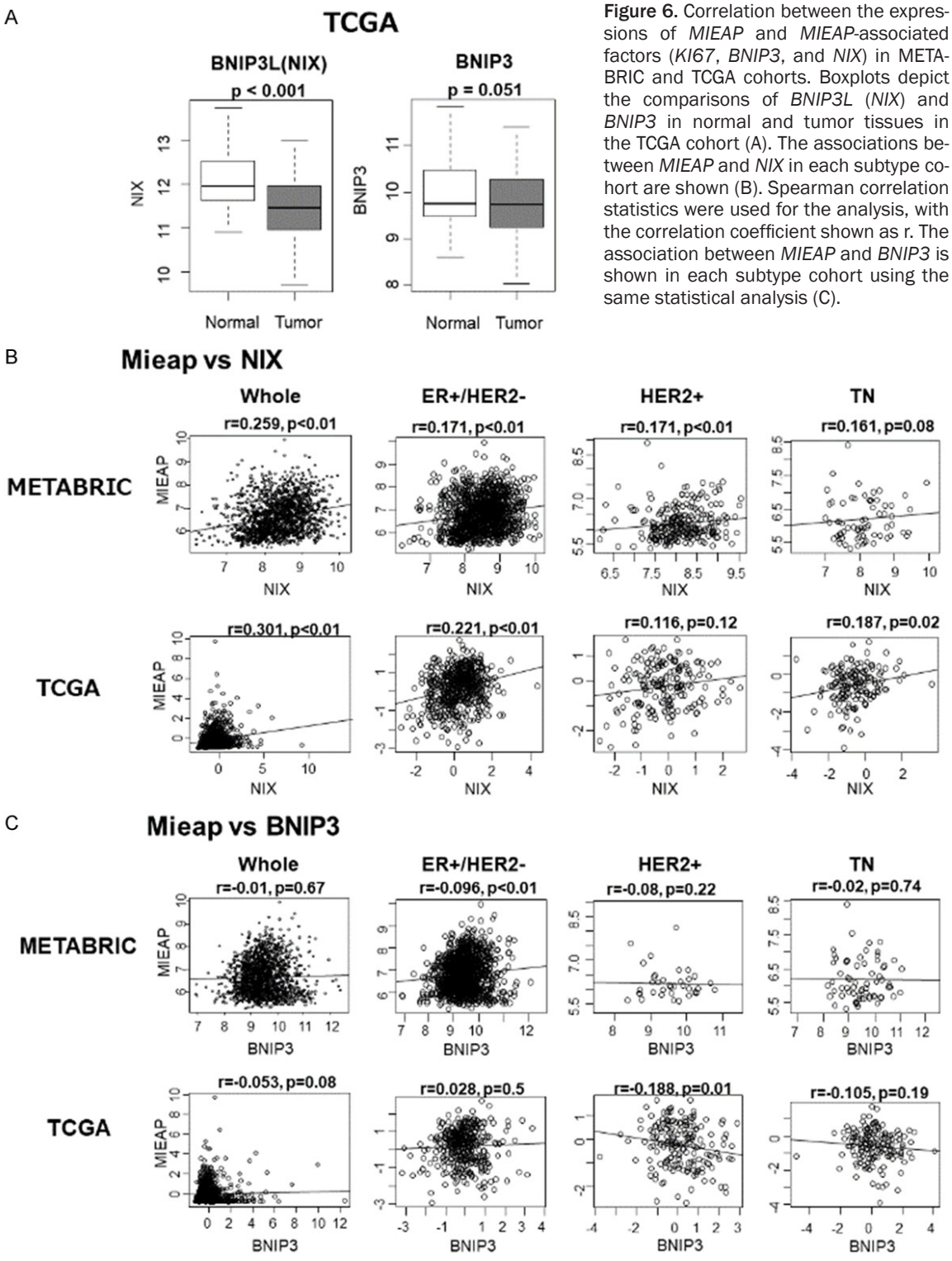

Figure 6. Correlation between the expressions of *MIEAP* and *MIEAP*-associated factors (*KI67*, *BNIP3*, and *NIX*) in METABRIC and TCGA cohorts. Boxplots depict the comparisons of *BNIP3L* (*NIX*) and *BNIP3* in normal and tumor tissues in the TCGA cohort (A). The associations between *MIEAP* and *NIX* in each subtype cohort are shown (B). Spearman correlation statistics were used for the analysis, with the correlation coefficient shown as r. The association between *MIEAP* and *BNIP3* is shown in each subtype cohort using the same statistical analysis (C).

to shorter DFS in patients with primary BC. In the current study, we analyzed the association between *MIEAP* expression and prognosis using the METABRIC and TCGA cohorts. We found a better prognosis in *MIEAP*-high tumors than in *MIEAP*-low tumors, results that were consistent with those in our previous study [20]. In the METABRIC cohort, DFS and OS in *MIEAP*-high tumors were significantly longer than those in *MIEAP*-low tumors in the whole cohort and the luminal subtype. In the TCGA cohort, *MIEAP*-high tumors in the luminal subtype showed significantly longer DFS. Although it is not clear why *MIEAP*-high tumors led to better prognosis, particularly in the luminal subtype, we can speculate on several factors: (1) the *MIEAP* expression level was higher in the luminal subtype than in the HER2+ or TN subtypes, suggesting that the former may contain a large population with better prognosis (Figure S1); (2) in the TCGA cohort, the *TP53*-mutation rate of BC was lower in the luminal subtype than in the HER2+ and TN subtypes [22], suggesting that the former may include a population expected to have a better prognosis; (3) *MIEAP*-low tumors, particularly in the luminal subtype, were significantly enriched in cell cycle- and proliferation-associated gene sets, suggesting that they might proliferate rapidly and lead to worse prognosis; and (4) the p53/*MIEAP*-MQC pathway was impaired by methylation of the *MIEAP* promoter, probably causing worse prognosis, particularly in the luminal subtype. Our previous study demonstrated that the *MIEAP* promoter was methylated in all luminal B type BCs, and that all patients with impairment of the p53/*MIEAP*-MQC pathway belonged to aggressive phenotypes such as luminal B, TN, or HER2+ subtypes [20].

In this study, we identified two features of *MIEAP* through GSEA. First, cell cycle- and proliferation-related gene sets were enriched in *MIEAP*-low tumors (**Figure 3**), and the data suggest the strong association of *MIEAP* with tumor progression. In estimating GSEA, we controlled the proportion of false positives by calculating the FDR corresponding to each NES. As shown in **Figure 3**, our study identified many negative NESs, suggesting that *MIEAP*-low tumors enriched the genes included in the gene set of interest. For instance, *MIEAP*-low tumors enriched the gene sets associated with cell proliferation, such as Myc Targets V1, Myc Targets V2, E2F targets, G2M checkpoints, and mTORC1 signaling. These results indicated that the downregulation of *MIEAP* is associated with increased cell cycle and cell proliferation, which may lead to tumor progression. This cancer biology may explain why patients with *MIEAP*-low tumors had worse survival outcomes than those with *MIEAP*-high tumors. Second, we found an association between *MIEAP* and mitochondria-associated gene sets. Several gene sets related to oxidative phosphorylation, glycolysis, ROS production, and UP response were significantly enriched among *MIEAP*-low tumors in some BC subtypes, particularly in the TCGA cohort. Gene sets associated with ROS production and UP response were enriched in both cohorts (**Figure 5**). These data suggest that *MIEAP* is strongly associated with the response to cell stress by the mitochondria. As we had already reported, *MIEAP* plays an important role in MQC. Although we found the clinical relevance of *MIEAP* expression in BC using two independent algorithms, this study still has some limitations: (1) our analysis was retrospective and limited to the measurement of gene expression, and we cannot, therefore, exclude statistical bias; and (2) tumor or normal samples might contain various types of cells with both epithelial and stromal components.

To our knowledge, this is the first study to demonstrate the association between *MIEAP* expression and survival in patients with luminal type BC using large-scale cohorts. Although we believe that our *in silico* approach is a valuable tool to obtain a comprehensive view of human cancers in the clinical setting, it further emphasizes the importance of analyzing clinical specimens. In conclusion, we found that the mechanistic role of *MIEAP* is clinically relevant in the two independent cohorts. Specifically, *MIEAP* was found to be p53-dependent, and its downregulation was associated with advanced breast tumors. Moreover, *MIEAP*-high tumors demonstrated a favorable BC prognosis, particularly in the luminal subtype, because of *MIEAP* control over the cell cycle. Thus, MIEAP plays an essential role as a tumor suppressor in BC.

Acknowledgements

The authors thank Ms. Enya for technical assistance. This study was supported in part by the Japan Society for the Promotion of Science,

KAKENHI (grant numbers 17K10542 [MF], 20K08954 [MF], 24240117 [HA], 23659178 [HA], and 25670169 [HA]); the Ministry of Health, Labor and Welfare for the Practical Research for Innovative Cancer, H26-practical-general-001 (HA); the Japan Agency for Medical Research and Development (AMED) grant number 15ck0106006h0002 (HA); and the National Cancer Center Research and Development Fund, grant number 23-B-7 (HA). US NCI/NIH grant R01CA160688, R01CA250412, R37CA248018, and P30-CA016056 as well as Department of Defense-BCRP grant W81XWH-19-1-0674 (KT).

Disclosure of conflict of interest

None.

Address correspondence to: Dr. Manabu Futamura, Breast Surgery, Department of Surgery, Graduate School of Medicine, Gifu University, 1-1 Yanagido, Gifu 501-1194, Japan. Tel: +81-58-230-6000; Fax: +81-58-230-6236; E-mail: mfutamur@gifu-u.ac.jp

References

[1] Hollstein M, Sidransky D, Vogelstein B and Harris CC. p53 mutations in human cancers. Science 1991; 253: 49-53.

[2] Vogelstein B, Lane D and Levine AJ. Surfing the p53 network. Nature 2000; 408: 307-310.

[3] Tanaka H, Arakawa H, Yamaguchi T, Shiraishi K, Fukuda S, Matsui K, Takei Y and Nakamura Y. A ribonucleotide reductase gene involved in a p53-dependent cell-cycle checkpoint for DNA damage. Nature 2000; 404: 42-49.

[4] Kimura T, Gotoh M, Nakamura Y and Arakawa H. hCDC4b, a regulator of cyclin E, as a direct transcriptional target of p53. Cancer Sci 2003; 94: 431-436.

[5] Ohnishi S, Futamura M, Kamino H, Nakamura Y, Kitamura N, Miyamoto Y, Miyamoto T, Shinogi D, Goda O and Arakawa H. Identification of NEEP21, encoding neuron-enriched endosomal protein of 21 kDa, as a transcriptional target of tumor suppressor p53. Int J Oncol 2010; 37: 1133-1141.

[6] Cui H, Kamino H, Nakamura Y, Kitamura N, Miyamoto T, Shinogi D, Goda O, Arakara H and Futamura M. Regulation of apoptosis by p53-inducible transmembrane protein containing sushi domain. Oncol Rep 2010; 24: 1193-1200.

[7] Futamura M, Kamino H, Miyamoto Y, Kitamura N, Nakamura Y, Ohnishi S, Masuda Y and Arakawa H. Possible role of semaphorin 3F, a candidate tumor suppressor gene at 3p21.3, in p53-regulated tumor angiogenesis suppression. Cancer Res 2007; 67: 1451-1460.

[8] Miyamoto Y, Futamura M, Kitamura N, Nakamura Y, Baba H and Arakawa H. Identification of UNC5A as a novel transcriptional target of tumor suppressor p53 and a regulator of apoptosis. Int J Oncol 2010; 36: 1253-1260.

[9] Kern SE, Kinzler KW, Bruskin A, Jarosz D, Friedman P, Prives C and Vogelstein B. Identification of p53 as a sequence-specific DNA-binding protein. Science 1991; 252: 1708-1711.

[10] Hearnes JM, Mays DJ, Schavolt KL, Tang L, Jiang X and Pietenpol JA. Chromatin immunoprecipitation-based screen to identify functional genomic binding sites for sequence-specific transactivators. Mol Cell Biol 2005; 25: 10148-10158.

[11] Miyamoto Y, Kitamura N, Nakamura Y, Futamura M, Miyamoto T, Yoshida M, Ono M, Ichinose S and Arakawa H. Possible existence of lysosome-like organella within mitochondria and its role in mitochondrial quality control. PLoS One 2011; 6: e16054.

[12] Kitamura N, Nakamura Y, Miyamoto Y, Miyamoto T, Kabu K, Yoshida M, Futamura M, Ichinose S and Arakawa H. Mieap, a p53-inducible protein, controls mitochondrial quality by repairing or eliminating unhealthy mitochondria. PLoS One 2011; 6: e16060.

[13] Nunnari J and Suomalainen A. Mitochondria: in sickness and in health. Cell 2012; 148: 1145-1159.

[14] Matouschek A, Pfanner N and Voos W. Protein unfolding by mitochondria. The Hsp70 import motor. EMBO Rep 2000; 1: 404-410.

[15] Yang Y, Karakhanova S, Hartwig W, D'Haese JG, Philippov PP, Werner J and Bazhin AV. Mitochondria and mitochondrial ROS in cancer: novel targets for anticancer therapy. J Cell Physiol 2016; 231: 2570-2581.

[16] Warbueg O. The metabolism of carcinoma cells. Cancer Res 1925; 9: 148-163.

[17] Warburg O. On the origin of cance cells. Science 1956; 123: 309-314.

[18] Nakamura Y, Kitamura N, Shinogi D, Yoshida M, Goda O, Murai R, Kamino H and Arakawa H. BNIP3 and NIX mediate Mieap-induced accumulation of lysosomal proteins within mitochondria. PLoS One 2012; 7: e30767.

[19] Siegel RL, Miller KD, Fuchs HE and Jemal A. Cancer statistics, 2021. CA Cancer J Clin 2021; 71: 7-33.

[20] Gaowa S, Futamura M, Tsuneki M, Kamino H, Tajima JY, Mori R, Arakawa H and Yoshida K. Possible role of p53/Mieap-regulated mitochondrial quality control as a tumor suppressor in human breast cancer. Cancer Sci 2018; 109: 3910-3920.

[21] Curtis C, Shah SP, Chin SF, Turashvili G, Rueda OM, Dunning MJ, Speed D, Lynch AG, Samara-

jiwa S, Yuan Y, Gräf S, Ha G, Haffari G, Bashashati A, Russell R, McKinney S, Langerød A, Green A, Provenzano E, Wishart G, Pinder S, Watson P, Markowetz F, Murphy L, Ellis I, Purushotham A, Børresen-Dale AL, Brenton JD, Tavaré S, Caldas C and Aparicio S. The genomic and transcriptomic architecture of 2,000 breast tumours reveals novel subgroups. Nature 2012; 486: 346-352.

[22] Cancer Genome Atlas Network. Comprehensive molecular portraits of human breast tumours. Nature 2012; 490: 61-70.

[23] Tokumaru Y, Oshi M, Katsuta E, Yan L, Huang JL, Nagahashi M, Matsuhashi N, Futamura M, Yoshida K and Takabe K. Intratumoral adipocyte-high breast cancer enrich for metastatic and inflammation-related pathways but associated with less cancer cell proliferation. Int J Mol Sci 2020; 21: 5744.

[24] Tokumaru Y, Katsuta E, Oshi M, Sporn JC, Yan L, Le L, Matsuhashi N, Futamura M, Akao Y, Yoshida K and Takabe K. High expression of miR-34a associated with less aggressive cancer biology but not with survival in breast cancer. Int J Mol Sci 2020; 21: 3045.

[25] Oshi M, Tokumaru Y, Asaoka M, Yan L, Satyananda V, Matsuyama R, Matsuhashi N, Futamura M, Ishikawa T, Yoshida K, Endo I and Takabe K. M1 macrophage and M1/M2 ratio defined by transcriptomic signatures resemble only part of their conventional clinical characteristics in breast cancer. Sci Rep 2020; 10: 16554.

[26] Tokumaru Y, Oshi M, Katsuta E, Yan L, Satyananda V, Matsuhashi N, Futamura M, Akao Y, Yoshida K and Takabe K. KRAS signaling enriched triple negative breast cancer is associated with favorable tumor immune microenvironment and better survival. Am J Cancer Res 2020; 10: 897-907.

[27] American Joint Committee on Cancer. AJCC Cancer staging manual. 2021, Available online: https://cancerstaging.org/.

[28] Elston CW and Ellis IO. Pathological prognostic factors in breast cancer. I. The value of histological grade in breast cancer: experience from a large study with long-term follow-up. Histopathology 1991; 19: 403-410.

[29] Tsuneki M, Nakamura Y, Kinjo T, Nakanishi R and Arakawa H. Mieap suppresses murine intestinal tumor via its mitochondrial quality control. Sci Rep 2015; 5: 12472.

[30] Aas T, Børresen AL, Geisler S, Smith-Sørensen B, Johnsen H, Varhaug JE, Akslen LA and Lønning PE. Specific P53 mutations are associated with de novo resistance to doxorubicin in breast cancer patients. Nat Med 1996; 2: 811-814.

[31] Kamino H, Nakamura Y, Tsuneki M, Sano H, Miyamoto Y, Kitamura N, Futamura M, Kanai Y, Taniguchi H, Shida D, Kanemitsu Y, Moriya Y, Yoshida K and Arakawa H. Mieap-regulated mitochondrial quality control is frequently inactivated in human colorectal cancer. Oncogenesis 2016; 4: e181.

[32] Sano H, Futamura M, Gaowa S, Kamino H, Nakamura Y, Yamaguchi K, Tanaka Y, Yasufuku I, Nakakami A, Arakawa H and Yoshida K. p53/Mieap-regulated mitochondrial quality control plays an important role as a tumor suppressor in gastric and esophageal cancers. Biochem Biophys Res Commun 2020; 529: 582-589.

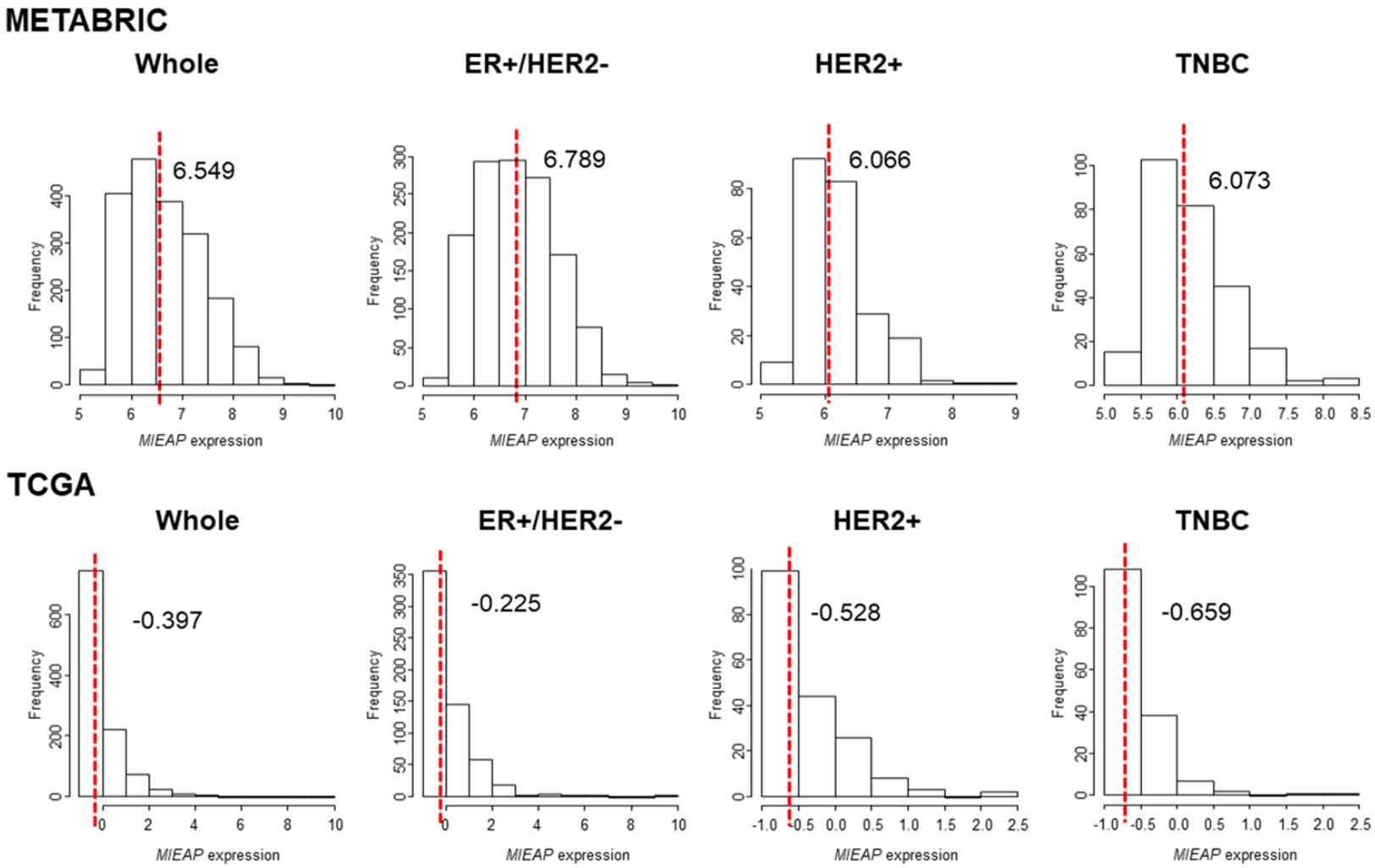

Figure S1. Expression level of *MIEAP* by histogram. Mieap expression in each breast cancer subtype was shown by METABRIC and TCGA. The red dotted lines in each histogram indicate the median cut-off value for each subtype. The patients were divided into *MIEAP*-high and *MIEAP*-low tumors according to the median gene expression levels in each cohort.